Damping rate of magnetohydrodynamic vortices at low magnetic Reynolds number

doi: 10.1063/1.2174056

Damping rate of magnetohydrodynamic vortices at low magnetic Reynolds number

Kazuyuki Ueno[a)]
Department of Aerospace Engineering, Tohoku University, Sendai 980-8579, Japan

René Moreau
Laboratoire EPM-MADYLAM, ENSHMG BP 95, 38402 Saint Martin d'Hères Cedex, France

(Received 20 June 2005; accepted 12 December 2005; published online 17 February 2006)

The damping rate of vortices in an electrically conducting fluid submitted to a uniform magnetic field is analyzed for a large Hartmann number Ha. The fluid is contained in a layer of constant thickness h, bounded by two insulating walls that are perpendicular to the magnetic field. The damping times and the eigenfunctions along the magnetic field are obtained from a linear eigenvalue problem. According to the damping times and these eigenfunctions, vortices are classified into several classes by the range of combinations of the mode number m in the magnetic field direction and the wave number k_{2D} in the plane perpendicular to the magnetic field. It is found that the damping rate of vortices in the range of $k_{2D} \sim [(m+\frac{1}{2})\pi \,\mathrm{Ha}]^{1/2} h^{-1}$ and $m=0,1,2$ is of the same order as that of large-scale two-dimensional vortices. This fact suggests that actual quasi-two-dimensional magnetohydrodynamic turbulent flows include not only $m=0$ but also higher-mode ($m \geqslant 1$) eigenfunctions of this wave-number range, although the eigenfunction of $m=0$ has a 30% variation and the higher-mode eigenfunctions change their sign along the magnetic field. © *2006 American Institute of Physics*. [DOI: 10.1063/1.2174056]

I. INTRODUCTION

Magnetohydrodynamic (MHD) turbulence at low magnetic Reynolds number has attracted significant attention over the past three decades and definite progress has been made along two fronts in that the tendency toward two dimensionality[1–4] and the development of the anisotropy[2] when an initial quasi-isotropic turbulence is suddenly submitted to a uniform magnetic field are now well understood. In addition, for a fluid that is located between two insulating Hartmann walls and is flowing in a quasi-two-dimensional (2D) turbulent regime due to the presence of a strong magnetic field, most of the main properties of the large-scale vortices have already been established.[5] However, a number of uncertainties remain with respect to the properties of the intermediate scale vortices and energy cascade in wave-number space. The purpose of the present study is to further clarify intermediate-scale MHD vortices at low magnetic Reynolds number.

We consider herein the unsteady flow of an incompressible electrically conducting fluid in the presence of a uniform magnetic field. The fluid domain is a layer of uniform thickness h bounded by two parallel insulating walls at $z=0$ and $z=h$, and the magnetic field $|\boldsymbol{B}|=B_0$ is oriented in the z direction (Fig. 1). We do not need more precision on either the geometry or the driving mechanisms, as the present discussion is an attempt to derive quite general properties. The physical properties of the fluid are such that the usual Reynolds number $\mathrm{Re}=U_0 L/\nu$ is much greater than unity, whereas the magnetic Reynolds number $\mathrm{Rm}=\mu\sigma U_0 L$ is much less than unity. Under such conditions, the fluid flow is highly turbulent and the induced magnetic field is negligible in comparison with the applied magnetic field. Moreover, the Hartmann number is much greater than unity:

$$\mathrm{Ha} = \sqrt{\frac{\sigma}{\rho\nu}} B_0 h \gg 1. \tag{1}$$

Such conditions are typical of liquid metal experiments performed on the laboratory scale. In the above expression, U_0 and L are the typical velocity and the maximum length scale of the existing vortices, respectively, ν is the kinematic viscosity, μ is the magnetic permeability, σ is the electric conductivity, and ρ is the density.

This kind of MHD turbulence, previously observed in experiments (see reviews by Lielausis[6] and Tsinober[7,8]), has been the subject of several theoretical investigations. Sommeria and Moreau[5] derived the necessary conditions for the turbulence to become quasi-2D and established a model equation that exhibits a linear damping term and takes into account both Joule dissipation and viscous dissipation within the Hartmann layer. Another property relevant to understanding the dynamics of MHD turbulence, discovered by Davidson,[9] is the invariance of the component of the angular momentum parallel to the magnetic field. In complement to the diffusion mechanism proposed by Sommeria and Moreau,[5] this invariance is also a key to understanding the tendency toward two dimensionality of the vortices in the direction of the magnetic field. Furthermore, several numerical simulations[10–16] that support the tendency toward anisotropy have been performed. Although they provide important new data that are very difficult to obtain experimentally, i.e., they provide data on the spatial distribution of instantaneous

[a)]Author to whom correspondence should be addressed. Electronic mail: ueno@cfd.mech.tohoku.ac.jp

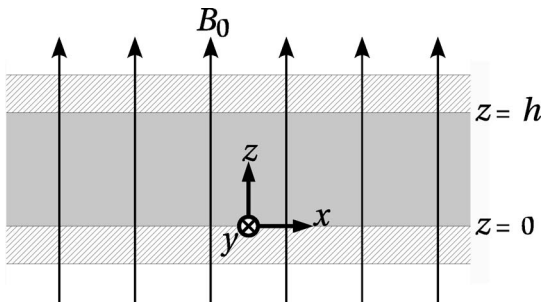

FIG. 1. Electrically conducting fluid layer bounded by two insulating walls perpendicular to a uniform magnetic field.

vorticity, a number of uncertainties on the transition from a three-dimensional (3D) regime to a quasi-2D regime remain.

Fourier transformation of the vorticity equation without any external energy supply is expressed as

$$\frac{\partial \hat{\omega}}{\partial t} = \hat{T} - \frac{\hat{\omega}}{\tau},$$

where $\hat{T}$ shows the nonlinear effect from the entire Fourier space, and $1/\tau$ is damping rate of the Fourier component $\hat{\omega}$. It is well known that the damping rate $1/\tau$ of vortices of nonconducting fluids is $\nu(k_x^2+k_y^2+k_z^2)$, where k_x, k_y, and k_z are components of the wave-number vector. Nevertheless, the damping rates of MHD vortices bounded by insulating Hartmann walls are not clear. The purpose of the present paper is to investigate the damping mechanisms and to derive the damping rates of quasi-2D vortices, which are likely to be present. Therefore, we disregard the nonlinear energy transfer between the different classes of vortices and take into account only the linear terms in the relevant equations. Such an analysis allows isolation of individual classes of vortices, each of which is characterized by two parameters: a wave number k_{2D} in the plane perpendicular to the magnetic field and a mode number m associated with the k_z component of the wave vector (see below for the full definition of these parameters). This purely linear investigation yields the damping rate of each class of vortices. The damping rate $1/\tau$ obtained by this linear problem is applicable to nonlinear problems, although $\partial\hat{\omega}/\partial t$ obtained by the linear problem is quite different from that obtained by nonlinear problems, in which the nonlinear effect $\hat{T}$ is important.

II. GOVERNING EQUATIONS

Boundary conditions on the insulating Hartmann walls are given by

$$\boldsymbol{u} = 0, \quad \boldsymbol{j}\cdot\boldsymbol{e}_z = 0 \quad \text{at } z = 0 \text{ and } h, \tag{2}$$

where the variables $\boldsymbol{u}$ and $\boldsymbol{j}$ are the velocity and current density, respectively. The damping of vortices is analyzed with the following set of linear equations:

$$\nabla\cdot\boldsymbol{u} = 0, \tag{3}$$

$$\frac{\partial \boldsymbol{u}}{\partial t} = -\frac{1}{\rho}\nabla p + \nu\nabla^2\boldsymbol{u} + \frac{1}{\rho}\boldsymbol{j}\times\boldsymbol{B}, \tag{4}$$

$$\nabla\cdot\boldsymbol{j} = 0, \tag{5}$$

$$\boldsymbol{j} = \sigma(-\nabla\phi + \boldsymbol{u}\times\boldsymbol{B}), \tag{6}$$

where the variables p and ϕ are the pressure and electric potential, respectively. In full MHD equations, $\boldsymbol{B}$ involves both the externally applied magnetic field and the induced magnetic field, which itself satisfies the induction equation. However, in the present study, as in most studies on MHD at low Rm, $\boldsymbol{B}$ is replaced by the external magnetic field $B_0\boldsymbol{e}_z$, because the ratio of the induced magnetic field to the external field is $O(\mathrm{Rm})$ and remains very small when $\mathrm{Rm}\ll 1$. This approximation is often referred to as the quasistatic approximation[17] of the induction equation. The first integral of the simplified induction equation reduces to Ohm's law (6) with $\boldsymbol{B}=B_0\boldsymbol{e}_z$. In this approximation, the induced magnetic field is the vector potential of the current density $\boldsymbol{j}$, although it does not explicitly appear in the above equation.

Following the procedure described by Sommeria and Moreau,[5] we replace the boundary conditions (2) at the wall by matching conditions for the core flow at the edge of the thin Hartmann layers:

$$\begin{aligned} &u_z \to 0, \quad \partial\phi/\partial z \to -\sqrt{\rho\nu/\sigma}\,\omega_z \quad \text{for } z\to 0,\\ &u_z \to 0, \quad \partial\phi/\partial z \to \sqrt{\rho\nu/\sigma}\,\omega_z \quad \text{for } z\to h. \end{aligned} \tag{7}$$

In these expressions, $\omega_z=\partial u_y/\partial x-\partial u_x/\partial y$ is the vorticity component in the direction of the magnetic field. The tangential components of the velocity u_x and u_y may allow some slip when $z\to 0$ or $z\to h$. Then, eliminating p and $\boldsymbol{j}$ yields

$$\frac{\partial \omega_z}{\partial t} = \nu\nabla_{2D}^2\omega_z - \frac{\sigma B_0}{\rho}(B_0\omega_z - \nabla_{2D}^2\phi), \tag{8}$$

$$\nabla^2\phi = B_0\omega_z, \tag{9}$$

where $\nabla_{2D}^2=\partial^2/\partial x^2+\partial^2/\partial y^2$ is the 2D Laplacian operator. Note that, in Eq. (8), we neglect $\nu\partial^2\omega_z/\partial z^2$ because we are concerned only with the core flow, whereby this term becomes negligible in comparison with the damping term $\sigma B_0\rho^{-1}(B_0\omega_z-\nabla_{2D}^2\phi)$.

Let us now introduce the 2D Fourier transformation

$$\hat{\omega}(t,z;k_x,k_y) = \frac{1}{(2\pi)^2}\int\int \omega_z(t,x,y,z) \times\exp[-i(k_x x + k_y y)]\mathrm{d}x\mathrm{d}y,$$

$$\omega_z(t,x,y,z) = \int\int \hat{\omega}(t,z;k_x,k_y)\exp[i(k_x x + k_y y)]\mathrm{d}k_x\mathrm{d}k_y,$$

where $i^2=-1$. Applying this transformation to Eqs. (7)–(9) yields

$$\begin{aligned} &\partial\hat{\phi}/\partial z \to -\sqrt{\rho\nu/\sigma}\,\hat{\omega} \text{ for } z\to 0,\\ &\partial\hat{\phi}/\partial z \to \sqrt{\rho\nu/\sigma}\,\hat{\omega} \text{ for } z\to h, \end{aligned} \tag{10}$$

$$\frac{\partial \hat{\omega}}{\partial t} = -\left(\frac{k_{2D}h}{\mathrm{Ha}}\right)^2\frac{\hat{\omega}}{\tau_J} - \frac{\hat{\omega}}{\tau_J} - \frac{k_{2D}^2\hat{\phi}}{B_0\tau_J}, \tag{11}$$

$$\frac{\partial^2 \hat{\phi}}{\partial z^2} - k_{2D}^2 \hat{\phi} = B_0 \hat{\omega}, \tag{12}$$

where we denote $k_{2D}^2 = k_x^2 + k_y^2$ and introduce the Joule time[5,18]

$$\tau_J = \frac{\rho}{\sigma B_0^2}. \tag{13}$$

III. EIGENVALUE PROBLEM

We express the solutions of linear equations (10)–(12) in the following form:

$$\hat{\omega} = f(z)\exp\left(-\frac{t}{\tau}\right), \quad \hat{\phi} = g(z)\exp\left(-\frac{t}{\tau}\right). \tag{14}$$

In any actual turbulent flow, the vorticity may not be damped in the above exponential function, because some nonlinear energy transfer is present. Nevertheless, it is highly instructive to estimate the dissipation of the turbulent energy by using the linear damping rate $1/\tau$. Substituting the above expressions into Eqs. (11) and (12) yields the following equation for $f(z)$:

$$\frac{d^2 f}{dz^2} + k_{2D}^2 \alpha^2 f = 0, \tag{15}$$

where

$$\alpha^2 = \left[1 + \left(\frac{k_{2D} h}{\mathrm{Ha}}\right)^2 - \frac{\tau_J}{\tau}\right]^{-1} - 1. \tag{16}$$

The relation between $g(z)$ and $f(z)$ is now

$$g(z) = -\frac{B_0}{k_{2D}^2 (1+\alpha^2)} f(z). \tag{17}$$

Substituting Eq. (14) into Eq. (10) yields the following boundary conditions:

$$\begin{aligned} \frac{df}{dz} &\to \frac{k_{2D}^2 h (1+\alpha^2)}{\mathrm{Ha}} f \quad \text{for } z \to 0, \\ \frac{df}{dz} &\to -\frac{k_{2D}^2 h (1+\alpha^2)}{\mathrm{Ha}} f \quad \text{for } z \to h. \end{aligned} \tag{18}$$

Equation (15) and boundary conditions (18) form an eigenvalue problem, which allows two sets of solutions. The eigenfunctions of the first set are the even functions of $z - h/2$:

$$f = \cos[k_z (z - h/2)],$$

where the eigenvalue $k_z \equiv \alpha k_{2D}$, which gives the wave number parallel to the magnetic field, is one of the roots of

$$\tan\left(\frac{k_z h}{2}\right) = \frac{(k_{2D}^2 + k_z^2) h}{k_z \, \mathrm{Ha}}.$$

The eigenfunctions of the second set are the odd functions of $z - h/2$:

$$f = \sin[k_z (z - h/2)],$$

where the eigenvalue $k_z \equiv \alpha k_{2D}$ is one of the roots of

$$\cot\left(\frac{k_z h}{2}\right) = -\frac{(k_{2D}^2 + k_z^2) h}{k_z \, \mathrm{Ha}}.$$

For each set, there is an infinite number of eigenvalues, which are given by the formula

$$\frac{k_{zm} h - m\pi}{2} = \arctan\left(\frac{(k_{2D}^2 + k_{zm}^2) h}{k_{zm} \mathrm{Ha}}\right) (m = 0, 1, 2, 3, \ldots). \tag{19}$$

Let us now call the integer m the mode number. The eigenvalues k_{zm} exist in the interval $m\pi < k_{zm} h < (m+1)\pi$, and, as a consequence, the eigenfunctions

$$f_m = \cos[k_{zm}(z - h/2)] \quad (m = 0, 2, 4, \ldots), \tag{20}$$

$$f_m = \sin[k_{zm}(z - h/2)] \quad (m = 1, 3, 5, \ldots) \tag{21}$$

have m zeros in the gap $0 < z < h$. Finally, it follows from Eq. (16) and this mode expansion that each vortex class has its own damping time τ_m, which may be expressed in terms of the wave number k_{2D} and of the mode number m:

$$\tau_m = \tau_J \left[\frac{k_{zm}^2}{k_{2D}^2 + k_{zm}^2} + \left(\frac{k_{2D} h}{\mathrm{Ha}}\right)^2\right]^{-1}. \tag{22}$$

If the initial condition $\hat{\omega}|_{t=0}$ is given by a function $\hat{\omega}_{\mathrm{init}}(z)$, then the general solution is obtained in the form of the following decomposition in eigenfunctions $f_m(z)$:

$$\hat{\omega}(t, z) = \sum_{m=0}^{\infty} \tilde{\omega}_m f_m(z) \exp\left(-\frac{t}{\tau_m}\right), \tag{23}$$

where the coefficients $\tilde{\omega}_m$ are given as follows (see the Appendix):

$$\begin{aligned} \tilde{\omega}_m = &\left(\frac{1}{h}\int_0^h \hat{\omega}_{\mathrm{init}}(z)\cos[k_{zm}(z - h/2)]\,dz \right. \\ &\left. - \frac{\hat{\omega}_{\mathrm{init}}(h) + \hat{\omega}_{\mathrm{init}}(0)}{\mathrm{Ha}}\cos(k_{zm} h/2)\right) \Bigg/ \\ &\left(\frac{1}{2} + \frac{k_{2D}^2 - k_{zm}^2}{k_{zm}^2 \, \mathrm{Ha}}\cos^2(k_{zm} h/2)\right) (m = 0, 2, 4, \ldots), \end{aligned} \tag{24}$$

$$\begin{aligned} \tilde{\omega}_m = &\left(\frac{1}{h}\int_0^h \hat{\omega}_{\mathrm{init}}(z)\sin[k_{zm}(z - h/2)]\,dz \right. \\ &\left. - \frac{\hat{\omega}_{\mathrm{init}}(h) - \hat{\omega}_{\mathrm{init}}(0)}{\mathrm{Ha}}\sin(k_{zm} h/2)\right) \Bigg/ \\ &\left(\frac{1}{2} + \frac{k_{2D}^2 - k_{zm}^2}{k_{zm}^2 \, \mathrm{Ha}}\sin^2(k_{zm} h/2)\right) (m = 1, 3, 5, \ldots). \end{aligned} \tag{25}$$

IV. DAMPING PROPERTIES

Let us now derive estimations of the eigenvalues for any arbitrary pair of parameters k_{2D} and m. We exclude small vortices $k_{2D} h \gtrsim \mathrm{Ha}$ and extremely high-mode numbers $m \gtrsim \mathrm{Ha}$, which are as small as the length scale of the Hartmann layer. Such small-scale disturbances do not correspond to the spectral range that is measurable in any experi-

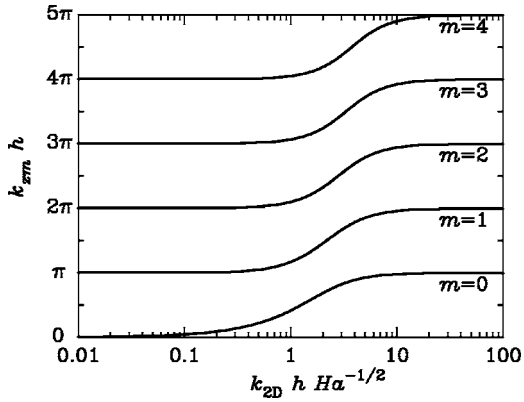

FIG. 2. Variation of the eigenvalues k_{zm} with respect to the wave number k_{2D} normalized by that of the classical parallel layer $h^{-1}\,\mathrm{Ha}^{1/2}$.

ment for $\mathrm{Ha}\gg 1$. Expanding Eqs. (19) and (22) with a small parameter $k_{zm}h\,\mathrm{Ha}^{-1}$ and neglecting the $O(k_{zm}h\,\mathrm{Ha}^{-1})$ terms, we obtain the following simplified relations:

$$\frac{k_{zm}h - m\pi}{2} = \arctan\left(\frac{k_{2D}^2 h}{k_{zm}\,\mathrm{Ha}}\right), \tag{26}$$

$$\frac{\tau_m - \tau_J}{\tau_H} = \frac{1}{k_{zm}h}\frac{k_{2D}^2 h/(k_{zm}\,\mathrm{Ha})}{1+[k_{2D}^2 h/(k_{zm}\,\mathrm{Ha})]^2}, \tag{27}$$

where the region of $k_{2D}^2 h/(k_{zm}\,\mathrm{Ha})$ is not restricted. Here,

$$\tau_H = \frac{h}{B_0}\sqrt{\frac{\rho}{\sigma\nu}} = \mathrm{Ha}\ \tau_J \tag{28}$$

is the Hartmann damping time.[5,18]

Figures 2 and 3 illustrate variations of $k_{zm}h$ and of $(\tau_m - \tau_J)/\tau_H$, which are compared for different values of the mode number m. The horizontal axes of Figs. 2 and 3 represent the wave number k_{2D} normalized by the thickness of the classical parallel layer[19] $h^{-1}\,\mathrm{Ha}^{1/2}$. The time scale τ_0 is a monotonic decreasing function of k_{2D}, whereas the other time scales τ_m for $m\geqslant 1$ are nonmonotonic functions of k_{2D} and have a maximum value at the wave number

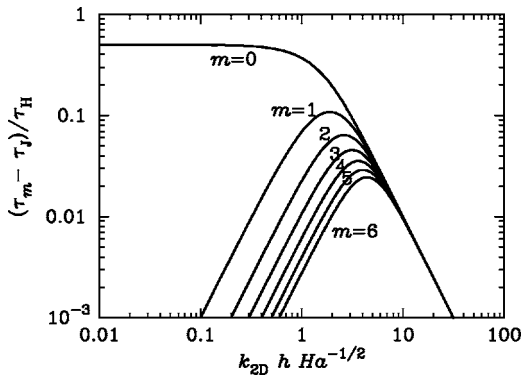

FIG. 3. Variation of the damping times τ_m with respect to the wave number k_{2D} normalized by that of the classical parallel layer $h^{-1}\,\mathrm{Ha}^{1/2}$. Here, Joule time τ_J is $\rho/(\sigma B_0^2)$ and Hartmann damping time τ_H is $(h/B_0)\sqrt{\rho/\sigma\nu}=\mathrm{Ha}\ \tau_J$.

TABLE I. Estimation of the eigenvalues k_{zm} and the eigenfunctions f_m.

	$k_{2D}\ll k_{2D}^*$	$k_{2D}\sim k_{2D}^*$ [a]	$k_{2D}\gg k_{2D}^*$
$k_{zm}h$	$m\pi$ [b]	$\left(m+\frac{1}{2}\right)\pi$	$(m+1)\pi$
$f_m(z)$	$\cos\frac{m\pi z}{h}$	$\cos\left[\left(m+\frac{1}{2}\right)\pi\left(\frac{z}{h}-\frac{1}{2}\right)\right]$ $(m=0,2,4,\ldots)$	$\sin\frac{(m+1)\pi z}{h}$
		$\sin\left[\left(m+\frac{1}{2}\right)\pi\left(\frac{z}{h}-\frac{1}{2}\right)\right]$ $(m=1,3,5,\ldots)$	

[a] $k_{2D}^*=\sqrt{(m+\frac{1}{2})\pi\,\mathrm{Ha}}/h$.
[b] $k_{z0}h=k_{2D}h\sqrt{2/\mathrm{Ha}}$ when $k_{2D}\ll k_{2D}^*$.

$$k_{2D}^* = \frac{1}{h}\sqrt{\left(m+\frac{1}{2}\right)\pi\,\mathrm{Ha}}. \tag{29}$$

Beyond the wave number k_{2D}^*, the eigenvalue k_{zm} increases from $m\pi$ to $(m+1)\pi$. We refer to k_{2D}^* as the matching wave number.

Table I describes the asymptotic behavior of the eigenvalues k_{zm} and the eigenfunctions $f_m(z)$ obtained from Eqs. (26), (20), and (21). This table also provides k_{zm} and $f_m(z)$ at the matching wave number k_{2D}^*. Furthermore, Table II provides the damping times τ_m obtained from Eq. (27), which are classified into several classes by the range of combinations of k_{2D} and m. The results given in these tables are discussed below for each class of vortices.

A. Large-scale vortices: $k_{2D}h\lesssim 1$

The wavelength of vortices of this class is greater than the fluid layer depth h. Thus, all of the higher-mode vortices $(m\geqslant 1)$ are oblate. The profile of the eigenfunction $f_0(z)$ is z independent. The damping time τ_0 is a half of the Hartmann damping time τ_H, which is much longer than τ_J. These large-scale wall-to-wall long-life vortices are exactly 2D, as suggested by quasi-2D MHD flow experiments.[6,8,18,20,21] The damping time of oblate vortices in this class $(m\geqslant 1,\ k_{2D}h \lesssim 1)$ is the Joule time τ_J, which is much shorter than τ_H. Consequently, such vortices are rapidly damped or do not exist from the beginning.

B. Medium-scale vortices: $1\lesssim k_{2D}h\ll[(m+\frac{1}{2})\pi\,\mathrm{Ha}]^{1/2}$

The wavelength of vortices of this class is smaller than h but greater than the matching scale. The profile of $f_0(z)$ is z independent and τ_0 is half of τ_H, as in the case of the large-scale vortices. The profiles of $f_m(z)$ for higher modes $(m\geqslant 1)$ are sinusoidal functions with a maximum at the outer edge of the core flow, as shown in Fig. 4. If vortices are prolate, then its damping time is much shorter than τ_H and much longer than τ_J. These vortices are the "quantized eddies" predicted by Sommeria and Moreau.[5] Quasi-2D MHD flow may be established after these vortices are damped. Note that the "quantized eddies" are found only in the

TABLE II. Damping times τ_m and their classification.

	Large scale ($k_{2D}h \lesssim 1$)	Medium scale ($1 \lesssim k_{2D}h \ll k_{2D}^* h$)	Matching scale ($k_{2D} \sim k_{2D}^*$)[a]	Extremely small scale ($k_{2D} \gg k_{2D}^*$)
Wall-to-wall ($m=0$)	$\frac{1}{2}\tau_H$ [b]	$\frac{1}{2}\tau_H$	$\frac{1}{\pi}\tau_H$	τ_ν [c]
Prolate ($1 \lesssim m \ll k_{2D}h$)	—	$\left(\frac{k_{2D}h}{m\pi}\right)^2 \tau_J$	$\frac{1}{(2m+1)\pi}\tau_H$	τ_ν
Isotropic ($m\pi \sim k_{2D}h$)	—	$2\tau_J$	—	—
Oblate ($m \gg k_{2D}h$)	τ_J [d]	τ_J	—	—

[a] $k_{2D}^* = \sqrt{(m+\frac{1}{2})\pi\,\mathrm{Ha}}/h$.
[b] Hartmann damping time: $\tau_H = (h/B_0)\sqrt{\rho/\sigma\nu} = \mathrm{Ha}\,\tau_J$.
[c] viscous damping time: $\tau_\nu = 1/(\nu k_{2D}^2) = (\mathrm{Ha}/k_{2D}h)^2 \tau_J$.
[d] Joule time: $\tau_J = \rho/(\sigma B_0^2)$.

medium-scale vortices $1 \lesssim k_{2D}h \ll k_{2D}^* h$, whereas all of the large-scale higher-mode vortices ($k_{2D}h \lesssim 1$, $m \geqslant 1$) are rapidly damped in a short time τ_J.

If medium-scale vortices are isotropic or oblate, then their damping time is on the order of τ_J. Consequently, such vortices are rapidly damped or do not exist from the beginning. This is the source of anisotropy of MHD turbulent flows.

C. Matching scale vortices: $k_{2D}h \sim [(m+\frac{1}{2})\pi\,\mathrm{Ha}]^{1/2}$

The center of the wave-number range of this class is the matching wave number $k_{2D}^* = [(m+\frac{1}{2})\pi\,\mathrm{Ha}]^{1/2} h^{-1}$. The wavelength of this class depends on the mode number m and is of the same order as the classical parallel layer[19] when $0 \leqslant m \lesssim 10$.

In this class, the series τ_m does not have an exceedingly large jump between τ_0 and τ_1, which is in contrast with large- and medium-scale vortices. The damping times for $m=0,1,2$ are of the same order as τ_0 of the large-scale wall-to-wall vortices. This suggests that actual quasi-2D MHD turbulent flows include not only $m=0$ but also the higher-mode ($m \geqslant 1$) eigenfunctions of the matching scale vortices.

The profiles of $f_m(z)$ are shown in Fig. 5. Even $f_0(z)$ has a 30% variation along the magnetic field. This sinusoidal distribution is very close to the parabolic distribution predicted by Pothérat *et al.*[22] using an asymptotic expansion in terms of the two small parameters Ha^{-1} and $N^{-1} = \mathrm{Re}/\mathrm{Ha}^2$.

D. Extremely small-scale vortices: $[(m+\frac{1}{2})\pi\,\mathrm{Ha}]^{1/2} \ll k_{2D}h \ll \mathrm{Ha}$

The vortices in this class are characterized by the fact that τ_m is independent of the mode number m and $\tau_m = \tau_\nu = 1/(\nu k_{2D}^2) = (\mathrm{Ha}/k_{2D}h)^2 \tau_J$ is much smaller than τ_H. This suggests that the preexisting extremely small vortices are rapidly damped. These vortices likely no longer dissipate energy if the energy cascade is toward the large scale.

Note also that $f_m(z)$ approaches the limit 0 at the outer edge of the core flow, as shown in Fig. 6. This suggests that these extremely small vortices have no Hartmann layers and may be considered as ordinary hydrodynamic vortices rather

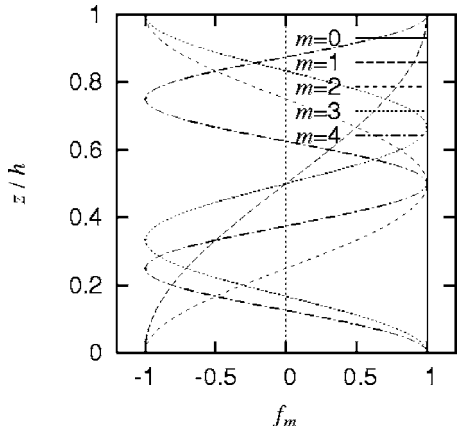

FIG. 4. Profiles of the eigenfunctions $f_m(z)$ for the medium-scale vortices $1 \lesssim k_{2D}h \ll [(m+\frac{1}{2})\pi\,\mathrm{Ha}]^{1/2}$.

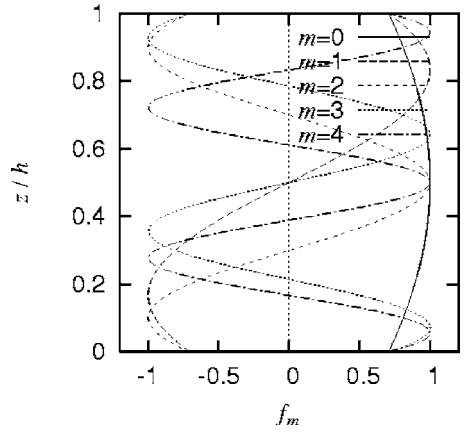

FIG. 5. Profiles of the eigenfunctions $f_m(z)$ for the matching scale vortices $k_{2D}h \sim [(m+1/2)\pi\,\mathrm{Ha}]^{1/2}$, the length scale for $0 \leqslant m \lesssim 10$ of which is on the same order as the classical parallel layer.

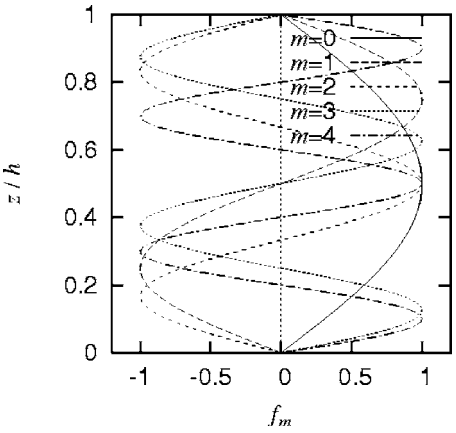

FIG. 6. Profiles of the eigenfunctions $f_m(z)$ for the extremely small-scale vortices $[(m+1/2)\pi \mathrm{Ha}]^{1/2} \ll k_{2D}h \ll \mathrm{Ha}$.

than MHD vortices. In addition, it is difficult to detect these vortices by measuring the potential on the wall, if they exist.

V. VORTICES IN QUASI-2D TURBULENT FLOWS

In the last section, vortices are classified and their damping time is clarified, as shown in Table II. According to these results, each time scale in a typical laboratory experiment[18] may be calculated as shown in Table III. In the case of $B_0=5.0$ (T), time scales are clearly divided into two groups. The first group consists of the large-scale wall-to-wall vortices, the medium-scale wall-to-wall vortices, and the matching scale vortices, while the second group consists of the medium-scale quantized vortices, the extremely small-scale vortices, the isotropic vortices, and the oblate vortices. Quasi-2D MHD flow includes the vortices of the first group.

In previous studies of quasi-2D MHD turbulence for large Hartmann number and small magnetic Reynolds number,[2–9] a great deal of attention has been given to the large-scale and medium-scale vortices. Nevertheless, the results of this study suggest that the matching scale vortices require a certain degree of attention, until it is clear whether the matching scale vortices are important with respect to the energy cascade.

This uncertainty may be clarified by numerical simulations that have sufficient resolution for the matching scale vortices

$$k_{2D}^2 \simeq \sqrt{\sigma/\rho\nu}B_0 k_z. \tag{30}$$

Numerical simulations satisfying the resolution of

$$\max(k_z) \sim \max(k_{2D}) \gtrsim \sqrt{\sigma/\rho\nu}B_0 \tag{31}$$

resolve all the matching scale vortices. The right-hand side $\sqrt{\sigma/\rho\nu}B_0$ is the wave number in a particular case of

TABLE III. Typical magnitude of the time scales in laboratory experimental conditions; $B_0=0.50$ or 5.0 (T), $h=0.01$ (m); physical properties of mercury: $\sigma=1.04\times10^6$ (S/m), $\rho=13.546\times10^3$ (kg/m^3), $\nu=1.15\times10^{-7}$ (m^2/s).

	$B_0=0.5$ (T) (Ha=130)		$B_0=5.0$ (T) (Ha=1300)	
	ℓ_{2D} (m)[a]	τ (s)	ℓ_{2D} (m)	τ (s)
Large-scale wall-to-wall vortices	0.10	3.4 ($\tau_{tu}\simeq1.0$[b])	0.10	0.34 ($\tau_{tu}\simeq1.0$)
Medium-scale wall-to-wall vortices	7.0×10^{-3}	3.4	5.0×10^{-3}	0.34
Parallel layer	5.5×10^{-3}	—	1.7×10^{-3}	—
Matching scale vortices	$\frac{4.4\times10^{-3}}{\sqrt{2m+1}}$	$\frac{2.1}{2m+1}$	$\frac{1.4\times10^{-3}}{\sqrt{2m+1}}$	$\frac{0.21}{2m+1}$
Medium-scale quantized vortices	7.0×10^{-3}	$\frac{0.41}{m^2}$	5.0×10^{-3}	$\frac{8\times10^{-3}}{m^2}$
Extremely small-scale vortices	8.0×10^{-4}	0.14	1.0×10^{-4}	2.2×10^{-3}
Hartmann layer	4.8×10^{-4}	—	4.8×10^{-5}	—
Isotropic vortices	$\lesssim$0.01	0.10	$\lesssim$0.01	1.0×10^{-3}
Oblate vortices	$\lesssim$0.01	0.05	$\lesssim$0.01	0.5×10^{-3}

[a]$\ell_{2D}=2\pi/k_{2D}$.
[b]Turnover time: $\tau_{tu}=\ell_{2D\,max}/U_0$. Here, we substitute $\ell_{2D\,max}\simeq0.10$ (m) and $U_0\simeq0.10$ (m/s) that correspond to a driving current $I\simeq10$ (A).

$\tau_H/[(2m+1)\pi] \sim \tau_J \sim \tau_\nu$. It is also the wave number of the Hartmann layer, which is excluded in the main part of the present study. If the results of a numerical simulation show that the energy cascade terminates at some wave number on $k_{2D}^2 \simeq \sqrt{\sigma/\rho\nu}B_0 k_z$, then this matching scale vortex is quite important and plays a similar role to that of the Kolmogorov scale vortex in nonconducting fluid flows. On the other hand, if the energy cascade terminates at some wave number out of $k_{2D}^2 \simeq \sqrt{\sigma/\rho\nu}B_0 k_z$ or if there is no energy cascade to large wave number, then the matching scale vortices are not important. If vortices at $k \sim \sqrt{\sigma/\rho\nu}B_0$ have turbulent energy, then the resolution of the simulation is not yet sufficient. In such a case, subgrid-scale models of large eddy simulation developed for nonconducting fluids[16] may be applicable to vortices of $k \gg \sqrt{\sigma/\rho\nu}B_0$. However, even if a subgrid-scale model is introduced as a large eddy simulation, a grid resolution satisfying Eq. (31) is recommended, because it remains unclear as to whether such subgrid-scale models are applicable to vortices of $k \lesssim \sqrt{\sigma/\rho\nu}B_0$.[10]

In addition to the sufficient resolution, a careful post-analysis is also required, which should exhibit the energy spectrum and the energy transfer function focused on the matching scale vortices.

VI. CONCLUSION

The damping rate of vortices in an electrically conducting fluid layer bounded by two insulating walls and submitted to a uniform magnetic field was investigated. The damping times τ_m and the eigenfunctions $f_m(z)$ along the magnetic field were obtained from a linear eigenvalue problem. A decomposition in eigenfunctions allows the vortices to be characterized by their wave number k_{2D} in the plane perpendicular to the magnetic field and by a mode number m in the magnetic field direction. According to τ_m and $f_m(z)$, vortices are classified into several classes that are specified by the range of combination of k_{2D} and m.

At the matching wave number $k_{2D}^* = [(m+\frac{1}{2})\pi\,\mathrm{Ha}]^{1/2}h^{-1}$, τ_m takes the maximum value, except for τ_0. The wavelength of the matching scale vortices for $0 \leqslant m \lesssim 10$ is of the same order as the classical parallel layer and the damping time $\tau_m = \tau_H/[(2m+1)\pi]$ for $m=0,1,2$ is of the same order as the large-scale wall-to-wall vortices $\tau_H/2$. This suggests that actual quasi-2D MHD turbulent flows include not only $m=0$ but also the higher-mode ($m \geqslant 1$) eigenfunctions of the matching scale vortices, although the eigenfunction $f_0(z)$ has a 30% variation and the higher-mode eigenfunctions $f_m(z)$ change their signs along the magnetic field.

The damping rate $1/\tau_m$ derived from this analysis may be useful to understand the nonlinear energy transfer present in such quasi-2D turbulent flows, because the comparison between the damping time and the energy transfer time is key to determining how the energy is distributed in the different Fourier modes. In particular, if a quasisteady regime is likely to be present, then the local equality between these time scales may impose the spectral law.

The results of the present study suggest the matching scale vortices require a certain degree of attention. Numerical simulations satisfying the resolution of $\max(k_z) \sim \max(k_{2D}) \gtrsim \sqrt{\sigma/\rho\nu}B_0$ are expected to clarify the role of the matching scale vortices in the energy cascade.

ACKNOWLEDGMENTS

The authors would like to thank Dr. Yves Delannoy and Professor Shinichi Kamiyama for their fruitful discussions.

APPENDIX: INTEGRAL OF PRODUCTS OF TWO EIGENFUNCTIONS

When m is an odd integer and n is an even integer, the integral of products of two eigenfunctions (20) and (21) are

$$\frac{1}{h}\int_0^h \sin\left[k_{zm}\left(z-\frac{h}{2}\right)\right]\cos\left[k_{zn}\left(z-\frac{h}{2}\right)\right]\mathrm{d}z = 0.$$

When both m and n are even, Eq. (19) gives the relations $\sin(k_{zm}h/2) = \cos(k_{zm}h/2)(k_{2D}^2+k_{zm}^2)h/(k_{zm}\,\mathrm{Ha})$ and $\sin(k_{zn}h/2) = \cos(k_{zn}h/2)(k_{2D}^2+k_{zn}^2)h/(k_{zn}\,\mathrm{Ha})$. Taking these relations into account, we obtain

$$\frac{1}{h}\int_0^h \cos\left[k_{zm}\left(z-\frac{h}{2}\right)\right]\cos\left[k_{zn}\left(z-\frac{h}{2}\right)\right]\mathrm{d}z = \frac{2}{\mathrm{Ha}}\cos\frac{k_{zm}h}{2}\cos\frac{k_{zn}h}{2} + \delta_{mn}\left(\frac{1}{2}+\frac{k_{2D}^2-k_{zn}^2}{k_{zn}^2\mathrm{Ha}}\cos^2\frac{k_{zn}h}{2}\right).$$

When both m and n are odd, Eq. (19) gives the relations $\cos(k_{zm}h/2) = -\sin(k_{zm}h/2)(k_{2D}^2+k_{zm}^2)h/(k_{zm}\,\mathrm{Ha})$ and $\cos(k_{zn}h/2) = -\sin(k_{zn}h/2)(k_{2D}^2+k_{zn}^2)h/(k_{zn}\,\mathrm{Ha})$. Taking these relations into account, we obtain

$$\frac{1}{h}\int_0^h \sin\left[k_{zm}\left(z-\frac{h}{2}\right)\right]\sin\left[k_{zn}\left(z-\frac{h}{2}\right)\right]\mathrm{d}z = \frac{2}{\mathrm{Ha}}\sin\frac{k_{zm}h}{2}\sin\frac{k_{zn}h}{2} + \delta_{mn}\left(\frac{1}{2}+\frac{k_{2D}^2-k_{zn}^2}{k_{zn}^2\,\mathrm{Ha}}\sin^2\frac{k_{zn}h}{2}\right).$$

[1] S. Chandrasekhar, *Hydrodynamic and Hydromagnetic Stability* (Clarendon, Oxford, 1961), pp. 157–159.
[2] H. K. Moffatt, "On the suppression of turbulence by a uniform magnetic field," J. Fluid Mech. **28**, 571 (1967).
[3] R. Moreau, "On magnetohydrodynamic turbulence," in *Proceedings of the Symposium on Turbulence in Fluids and Plasmas* (Polytechnic Institute of Brooklyn, 1968), p. 359.
[4] A. Alemany, R. Moreau, P. L. Sulem, and U. Frisch, "Influence of an external magnetic field on homogeneous MHD turbulence," J. Mec. **18**, 277 (1979).
[5] J. Sommeria and R. Moreau, "Why, how, and when, MHD turbulence becomes two-dimensional," J. Fluid Mech. **118**, 507 (1982).
[6] O. Lielausis, "Liquid metal magnetohydrodynamics," At. Energy Rev. **13**, 527 (1975).
[7] A. Tsinober, "Magnetohydrodynamic turbulence," Magnetohydrodynamics (N.Y.) **11**, 5 (1975).
[8] A. Tsinober, "MHD flow drag reduction," Prog. Astronaut. Aeronaut. **123**, 327 (1990).
[9] P. Davidson, "The role of angular momentum in the magnetic damping of turbulence," J. Fluid Mech. **336**, 123 (1997).
[10] Y. Shimomura, "Large eddy simulation of magnetohydrodynamic turbulent channel flows under a uniform magnetic field," Phys. Fluids A **3**, 3098 (1991).
[11] K. Ueno, K. Saito, and S. Kamiyama, "Three-dimensional simulation of

MHD flow with turbulence," JSME Int. J., Ser. B **44**, 38 (2001) [Trans. Jpn. Soc. Mech. Eng., Ser. B **65**, 2976 (1999)].
[12] B. Mück, C. Günther, U. Müller, and L. Bühler, "Three-dimensional MHD flows in rectangular ducts with internal obstacles," J. Fluid Mech. **418**, 265 (2000).
[13] D. Lee and H. Choi, "Magnetohydrodynamic turbulent flow in a channel at low magnetic Reynolds number," J. Fluid Mech. **439**, 367 (2001).
[14] M. Hossain, "Inverse energy cascades in three-dimensional turbulence," Phys. Fluids B **3**, 511 (1991).
[15] O. Zikanov and A. Thess, "Direct numerical simulation of forced MHD turbulence at low magnetic Reynolds number," J. Fluid Mech. **358**, 299 (1998).
[16] B. Knaepen and P. Moin, "Large-eddy simulation of conductive flows at low magnetic Reynolds number," Phys. Fluids **16**, 1255 (2004).
[17] B. Knaepen, S. Kassinos, and D. Carati, "Magnetohydrodynamic turbulence at moderate magnetic Reynolds number," J. Fluid Mech. **513**, 199 (2004).
[18] K. Messadek and R. Moreau, "An experimental investigation of MHD quasi-two-dimensional turbulent shear flows," J. Fluid Mech. **456**, 137 (2002).
[19] J. C. R. Hunt and J. A. Shercliff, "Magnetohydrodynamics at high Hartmann number," Annu. Rev. Fluid Mech. **3**, 37 (1971).
[20] J. Sommeria, "Experimental study of the two-dimensional inverse energy cascade in a square box," J. Fluid Mech. **170**, 139 (1986).
[21] S. Sukoriansky, I. Zilberman, and H. Branover, "Experimental studies of turbulence in mercury flows with transverse magnetic fields," Exp. Fluids **4**, 11 (1986).
[22] A. Pothérat, J. Sommeria, and R. Moreau, "An effective two-dimensional model for MHD flows with transverse magnetic field," J. Fluid Mech. **424**, 75 (2000).